Interband transitions in $GaN_{0.02}As_{0.98-x}Sb_x/GaAs$ ($0<x\leqslant 0.11$) single quantum wells studied by contactless electroreflectance spectroscopy

R. Kudrawiec,* M. Gladysiewicz, and J. Misiewicz
Institute of Physics, Wrocław University of Technology, Wybrzeze Wyspianskiego 27, 50-370 Wrocław, Poland

H. B. Yuen, S. R. Bank, M. A. Wistey, H. P. Bae, and James S. Harris, Jr.
Solid State and Photonics Laboratory, Department of Electrical Engineering, 126X CISX, Via Ortega, Stanford University, Stanford, California 94305-4075, USA

(Received 27 December 2005; revised manuscript received 9 March 2006; published 14 June 2006)

Interband transitions in $GaN_{0.02}As_{0.98-x}Sb_x/GaAs$ single quantum wells (SQWs) with $0<x\leqslant 0.11$ have been investigated by contactless electroreflectance (CER). CER features related to the ground and excited state transitions have been observed and compared with those obtained from theoretical calculations, which were performed in the framework of the effective mass formalism model. It has been concluded that these SQWs are type I and the conduction band offset for this material system decreases from 80% to 50% when the Sb composition is increased from 0% to 11%. It shows that the band gap discontinuity for GaNAsSb/GaAs material system can be simply tuned by a change in Sb concentration.

DOI: 10.1103/PhysRevB.73.245413 PACS number(s): 78.67.De, 71.20.−b

I. INTRODUCTION

Dilute-nitride III-V compound semiconductors are of considerable research interest from both the fundamental and technological points of view.[1,2] In addition to GaInNAs, GaNAsSb appears to be a promising alloy for GaAs-based lasers operated at long wavelengths, i.e., at 1.3 and 1.55 μm. However, very few studies of GaNAsSb have been reported[3–13] since the initial proposal in 1999 (Ref. 3) and many fundamental optical properties of GaNAsSb are still unknown. One of the remaining unresolved issues with respect to electronic properties of GaNAsSb/GaAs quantum well (QW) structures involves the band gap discontinuity and its change with an increase in Sb composition. In the case of Sb-free QWs, i.e., GaNAs/GaAs QWs, many different results on the conduction band offset have been published to date.[14–24] Most researchers are in agreement that GaNAs/GaAs QW structures are type I and the conduction band offset for $GaN_{0.02}As_{0.98}/GaAs$ QWs is close to 80%.[23,24] It is expected that the incorporation of Sb atoms into a $GaN_{0.02}As_{0.98}/GaAs$ QW significantly influences the conduction and valence band offsets because GaAsSb/GaAs QWs are type II for electrons[5,25,26] or are type I with a very small conduction band offset.[27] Recently, we have shown that the conduction band offset equals 50% for $GaN_{0.02}As_{0.87}Sb_{0.11}/GaAs$ SQWs.[13] However, further investigation of GaNAsSb/GaAs QWs is still required. The aim of this paper is to study the optical transitions for a set of $GaN_{0.02}As_{0.98-x}Sb_x/GaAs$ SQWs with $0<x\leqslant 0.11$. In order to investigate the quantum well transitions we have applied contactless electroreflectance (CER) spectroscopy. This technique, similar to photoreflectance (PR) spectroscopy, is an excellent tool to investigate both the fundamental and higher order QW transitions.[28–33] Moreover, CER has a number of advantages over PR for the study of QW structures. CER does not require a laser as the pump beam and avoids the photoluminescence background due to this pump beam. Also, CER spectra are free of below band gap oscillation features, which are often observed in PR spectra, especially for GaAs-based structures grown on *n*-type GaAs substrates.[32] The analysis of CER data together with theoretical calculations makes it possible to determine material parameters such as the band gap discontinuity. Such procedures have been often applied in studies for different semiconductor structures.[30,31,33]

The focus of this paper is the application of CER spectroscopy to $GaN_{0.02}As_{0.98-x}Sb_x/GaAs$ single QWs (SQWs) with $0<x\leqslant 0.11$ in order to determine the energies of the interband transitions and to extract the conduction band offset for this system by matching experimental data with theoretical calculations performed within the effective mass approximation.

II. SAMPLES AND EXPERIMENT

The GaNAsSb/GaAs SQW samples prepared for this study were grown on semi-insulating (100) GaAs substrates by solid-source molecular beam epitaxy (MBE) in a Varian Mod Gen-II system. Details of the growth process are described elsewhere.[10,12] The SQW structure is composed of a 250 nm thick GaAs buffer layer, 50 nm thick GaAs:N layer with the nitrogen concentration of ~0.1%, 60 Å thick $GaN_{0.02}As_{0.98-x}Sb_x$ QW, and 50 nm thick GaAs cap layer. The GaAs:N layer is not an intentional part of the structure, but a result of the growth method used. The concentration of Sb atoms into $GaN_{0.02}As_{0.98-x}Sb_x$ layer for the three samples is 3%, 6%, and 11%, respectively. All samples were not annealed. The content of GaNAsSb layer and the width of QW were determined by secondary ion mass spectroscopy and high resolution x-ray diffraction (HRXRD) measurements as being close to the nominal values.

A conventional experimental set-up with a tungsten halogen lamp (150 *W*) as a probe light source, a 0.55 m monochromator and InGaAs *pin* photodiode was applied for obtaining CER spectra. Samples were mounted in a capacitor. The top electrode of the capacitor is a copper-wire mesh

which is semitransparent for light. This electrode was kept at a distance of 0.1–0.3 mm from the sample surface while the sample itself was fixed on the bottom copper electrode. A maximum peak-to-peak alternating voltage of ~0.9 kV was applied. The frequency of the ac voltage was 285 Hz. Phase sensitive detection of CER signal was made using a lock-in amplifier. Other relevant details of CER set-up are described in Refs. 28, 29, and 33.

III. THEORETICAL APPROACH

The calculations of QW energy levels have been performed within the framework of the effective mass approximation. The influence of strain on the band structure is taken into account, but excitonic effects are neglected. The biaxial strain was calculated based on the Pikus-Bir Hamiltonian[34] as is shown below.

For the E_0 critical point in GaNAsSb the hydrostatic component of the strain, δE_H, shifts the valence and conduction bands. This total shift corresponds to the change in the band gap energy due to a hydrostatic deformation, which is proportional to the deformation potential a, that is measured. The total shift should be divided between the valence and conduction bands proportionally to the potential constants a_V and a_C, where $a=a_V+a_C$. The shear component, δE_S, removes the valence band degeneracy, giving a separate E_{HH} (related to heavy holes) and E_{LH} (related to light holes). If the effect of the strain-induced coupling with the spin-orbit split band is negligible, the energy of conduction and valence bands can be expressed in terms of the unstrained value as

$$E_C = E_0 + \delta E_H^C, \tag{1a}$$

$$E_{HH} = E_0 + \delta E_H^V + \delta E_S, \tag{1b}$$

$$E_{LH} = E_0 + \delta E_H^V - \delta E_S + \cdots. \tag{1c}$$

The values of the δE_H^C, δE_H^V, and δE_S are given by following formulas:

$$\delta E_H^C = 2a^C \cdot \left(1 - \frac{C_{12}}{C_{11}}\right)\varepsilon, \tag{2a}$$

$$\delta E_H^V = 2a^V \cdot \left(1 - \frac{C_{12}}{C_{11}}\right)\varepsilon, \tag{2b}$$

$$\delta E_S = b \cdot \left(1 - 2\frac{C_{12}}{C_{11}}\right)\varepsilon, \tag{2c}$$

where ε is the strain in the plane of the interfaces, C_{11} and C_{12} are elastic stiffness constants, and b is the shear deformation potential, respectively. All the parameters have been obtained by linear interpolation between the parameters of a relevant binary semiconductor[35] according to Eq. (3),

$$Q(x,y) = y \cdot Q_{\mathrm{GaN}} + (1-x-y) \cdot Q_{\mathrm{GaAs}} + x \cdot Q_{\mathrm{GaSb}}, \tag{3}$$

where $Q_i=b_i$ or $C12_i$ (i=GaN, GaAs, and GaSb). The parameters of binary compounds used in our calculations are listed in Table I.

TABLE I. Room temperature binary material parameters used to calculate the strained ternary $GaN_{0.02}As_{0.98-x}Sb_x$ material parameters taken after Ref. 35.

Parameter (unit)	GaN	GaAs	GaSb
Heavy-hole mass m_{hh}/m_0	0.847	0.35	0.25
Light-hole mass m_{lh}/m_0	0.237	0.09	0.044
CB hydrostatic deformation potential a^C (eV)	−6.71	−7.17	−7.5
VB hydrostatic deformation potential a^V (eV)	−0.69	−1.16	−0.8
Shear deformation potential b (eV)	−2.0	−2.0	−2.0
Elastic constant C_{11} (GPa)	293	1221	884.2
Ealstic constant C_{12} (GPa)	159	566	402.6

The strain present in our samples has been determined directly by HRXRD measurements to be, respectively, $\varepsilon=-0.5\%$ for $GaN_{0.02}As_{0.87}Sb_{0.11}$/GaAs QWs, $\varepsilon=-0.06\%$ for $GaN_{0.02}As_{0.91}Sb_{0.06}$/GaAs QWs, and $\varepsilon=0.2\%$ for $GaN_{0.02}As_{0.95}Sb_{0.03}$/GaAs QWs. According to the band anticrossing model (BAC) model,[1,2,36] the influence of nitrogen localized states on the valence band structure is neglected. Hence, it can be assumed that the effective mass of light and heavy hole does not change significantly after adding of nitrogen atoms. Therefore the light and heavy hole masses are calculated according to Eq. (3) with effective masses of relevant binary semiconductors taken after Ref. 35. The electron effective mass has been assumed to be 0.09 m_0 after Ref. 8. This assumption indicates an increase in the electron effective mass in comparison to the N free sample. Note that such an electron effective mass is in accordance with the BAC model prediction.[1,2,36] We calculated that the electron effective for $GaN_{0.02}As_{0.98}$ is 0.1 m_0 with the BAC model. Other analyses also show that the electron effective mass for $GaN_{0.02}As_{0.98}$ is ~0.1 m_0. Unfortunately, BAC parameters for GaNAsSb are unknown and m_0 cannot be extracted from the BAC model. It is expected that incorporation of Sb atoms decreases the electron effective mass because it also decreases the band gap energy. The value of 0.09 m_0 in Ref. 8 has been determined for GaNAsSb/GaAs QW with 30% Sb and 1.5% N. Thus, we can expect that in our samples, the electron effective mass is between 0.09 m_0 and 0.01 m_0. In general, the electron effective mass in our samples can vary with the Sb content (decreases with the larger Sb content), but the change should be small since the total variation of Sb content is only 8%. Finally, we conclude that for these samples, the best approach is to calculate the energy levels with the same value of the electron effective mass, i.e., $m_e=0.09m_0$. It has been found that the BAC model with GaNAs parameters is insufficient to describe the GaNAsSb band gap. Therefore the band gap energy of the GaNAsSb layer has been adjusted to the experimental value of the QW ground state transition. The conduction- and valence-band offset, Q_C and Q_V, are defined as $Q_C=\frac{\Delta E_C}{(\Delta E_C+\Delta E_V)}$ and $Q_V=1-Q_C$, where ΔE_C and ΔE_V are the conduction- and valence-band discontinuities at the heterojunction. Note that in our calculations, we assume Q_C before taking into account the strain effects as it is shown in Fig. 1. In our calculations, the Q_C is treated as a free parameter.

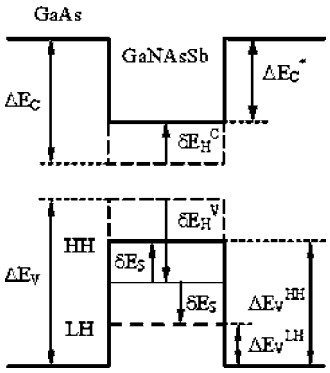

FIG. 1. The energy-band diagram in real space for a $GaN_{0.02}As_{0.98-x}Sb_x/GaAs$ SQW for the case of compression ($x > 0.05$). For the case of the tension ($x < 0.05$), all the energy shifts due to strains are in the opposite directions.

IV. RESULTS AND DISCUSSION

Figure 2 shows the CER spectra obtained from the $GaN_{0.02}As_{0.98-x}Sb_x/GaAs$ SQWs with different Sb concentrations. All CER spectra are dominated by a GaAs band gap bulklike signal at the energy of ~1.42 eV. This signal could be a superposition of CER resonances related to absorption in the GaAs cap and buffer layers. The contribution from the two signals can change from sample to sample due to different band bending at the surface and at the buffer/substrate interface. Therefore, the shape of GaAs signal is not exactly the same for the three samples.

In the case of $GaN_{0.02}As_{0.87}Sb_{0.11}/GaAs$ SQW, a CER feature related to the GaAs:N layer is observed at the energy of ~1.37 eV. This feature confirms the presence of an intermediate GaAs:N layer due to plasma ignition and stabilization prior to the QW. Such a feature has been observed in our previous PR study preformed for similar QW structures.[13,32,33] Note that the GaAs:N related transition is not observed for the two remaining SQWs. We believe that this phenomenon is associated with the lower amount of N in the intermediate layer.

Below the GaAs signal (in the case of the $GaN_{0.02}As_{0.87}Sb_{0.11}/GaAs$ SQW, below the GaAs:N related transition) CER features associated with the optical transitions in GaNAsSb/GaAs SQW are clearly observed. These features are analyzed using the low-field electromodulation Lorentzian line shape functional form[28,37]

$$\frac{\Delta R}{R}(E) = \mathrm{Re}\left[\sum_{j=1}^{n} C_j \cdot e^{i\cdot\vartheta_j}(E - E_j + i\cdot\Gamma_j)^{-m_j}\right], \qquad (4)$$

where n is the number of the optical transitions and spectral functions used in the fitting procedure, C_j and ϑ_j are the amplitude and phase of the line shape, and E_j and Γ_j are the energy and the broadening parameter of the transitions, respectively. The term m_j refers to the type of optical transitions in question: m_j=2, 2.5, and 3 for an excitonic transition, a three-dimensional one-electron transition, and a two-dimensional one-electron transition, respectively. We believe that the band-to-band character of the optical transition takes place for the investigated QWs at room temperature. Therefore, we assumed that m=3 for GaNAsSb/GaAs QW transitions. The fitting curves are shown by solid lines in Fig. 2 together with the modulus of the individual resonance obtained according to Eq. (2),

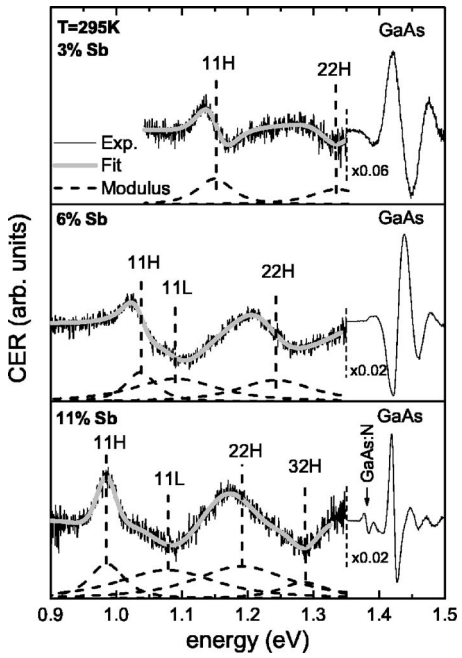

FIG. 2. Room temperature CER spectra of 60 Å $GaN_{0.02}As_{0.98-x}Sb_x/GaAs$ SQWs (thin solid line) with different Sb composition together with fitting curves (thick gray solid line) and the modulus of the individual lines (dashed lines).

$$\Delta\rho_j(E) = \frac{|C_j|}{[(E - E_j)^2 + \Gamma_j^2]^{m_j/2}} \qquad (5)$$

with parameters taken from the fit.

The identification of CER resonances was possible due to a series of calculations. The notation $nmH(L)$ denotes the transition between nth heavy hole (light hole) valence subband and mth conduction subband. The resonance at the lowest energy originates from the 11H transition, which is a fundamental transition for all SQW samples. In addition to the 11H transition, the CER spectra show an 11L transition (i.e., the lowest energy transition for light holes) and transitions between excited QW states. The 11L transition is typically not resolved for GaNAs/GaAs QWs (Refs. 23 and 24) primarily due to its lower intensity in comparison to the 11H transition and convolution with the 11H transition. However, the 11L transition has been observed many times for other QW systems,[38–40] especially compressively strained QWs. Thus, the 11L transition should be considered for GaNAsSb/GaAs QWs.

The procedure for correlating measured data with theory is described here. The QW transition energies were calculated as a function of Q_C using the approach described in the Sec. III. These energies were then compared with those found from CER spectra using a plot shown in Fig. 3. Here, the experimental transition energies are shown as horizontal dashed lines while those calculated are shown as solid

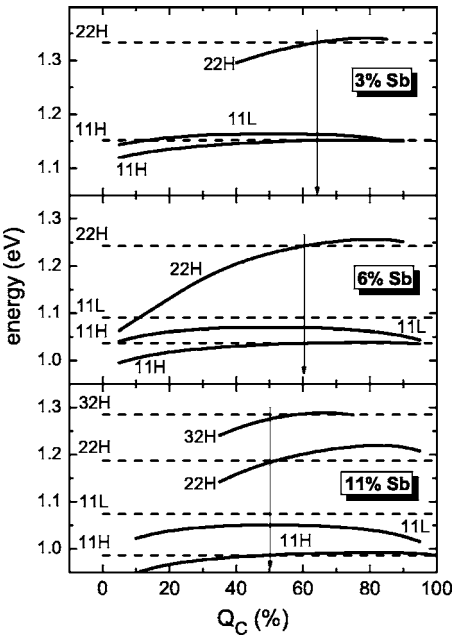

FIG. 3. Method used to achieve a match of theoretical QW transition energies (solid curves) with those found from fitting the CER spectra (horizontal dashed lines).

curves. Using this method, the optimal match between theory and experiment can be determined by comparing the data with calculated energies. Note that the accuracy of Q_C determination by this method is improved if additional QW transitions were observed, i.e., transitions related to excited states such as 22*H*, 32*H*, etc. Finally, we assumed that the Q_C changes linearly with the rise in Sb composition, as it is shown in Fig. 4. It has been determined that Q_C is 72% and 64% for $GaN_{0.02}As_{0.95}Sb_{0.03}$/GaAs and $GaN_{0.02}As_{0.92}Sb_{0.06}$/GaAs SQWs, respectively. Please note that in our calculations, we assume that the electron effective mass does not change with an increase in Sb concentration. This assumption can affect the conclusions relating to the Q_C value. If an electron effective mass which is too small is assumed, the determined conduction band offset is also too small. It is suspected that this effect is important for SQW samples with 3% of Sb. The assumed electron effective mass ($0.09\ m_0$)

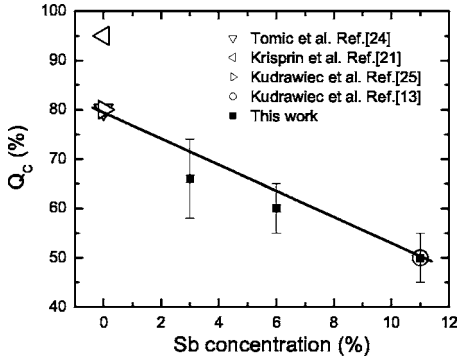

FIG. 4. Q_C determined for $GaN_{0.02}As_{0.98-x}Sb_x$/GaAs SQWs with $0<x<0.11$ together with literature data for $GaN_{0.02}As_{0.98}$/GaAs QWs and $GaN_{0.02}As_{0.77}Sb_{0.11}$/GaAs QWs.

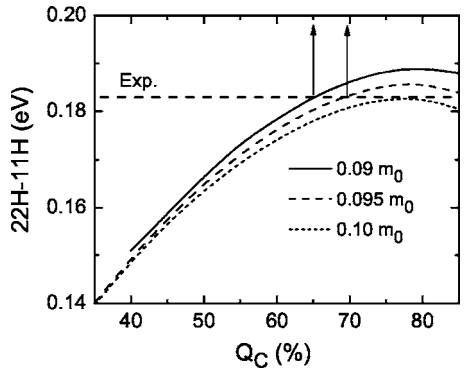

FIG. 5. Analysis of the Q_C in the $GaN_{0.02}As_{0.95}Sb_{0.03}$/GaAs SQW performed for various electron effective mass.

could be too low since the electron effective mass for the Sb-free SQW is higher than $0.09\ m_0$ (see the discussion in Sec. III) and Refs. 23, 24, and 41 and the incorporation of only 3% of Sb has negligible influence on the electron effective mass. Thus for this SQW, we have performed calculations with larger electron effective mass in order to estimate the error associated with different electron effective masses. Note that the change in the electron effective mass among the samples cannot be too large because the total variation in Sb content is only 8%. In order to find a reasonable limit for the increase in the electron effective mass, we examined the $GaAs_{1-x}Sb_x$ alloy. The effective mass for this alloy has been calculated after Eq. (3) and has been found to increase from $0.062\ m_0$ to $0.066\ m_0$ (less than 7%) with Sb content from 11% to 3%. We then assumed the limit electron effective mass increase in the $GaN_{0.02}As_{0.98-x}Sb_x$ alloy is similar (e.g., <10%). Figure 5 shows calculations performed for the SQW with 3% Sb for three different electron effective masses and various Q_C together with experimental data (horizontal dashed line). The energy difference between the 22*H* and 11*H* transitions is shown because the curves relating to different electron effective masses are more visible on such a figure. The electron effective masses are larger by 6% ($0.005\ m_0$) and 11% ($0.01\ m_0$) than the previously assumed value. It is clearly visible that the conduction band offset rises with the increase in the electron effective mass. For electron effective masses which are larger by 6%, the conduction band offset is close to 70%. This value agrees very well with the trend in Q_C shown in Fig. 4 by the thick line. It confirms the conclusion that the conduction band offset in GaNAsSb/GaAs SQW decreases with an increase in Sb concentration.

The depth of the electron (ΔE_C^*), light hole (ΔE_V^{LH}), and heavy hole (ΔE_V^{HH}) QWs obtained after the linear interpolation between Q_C for Sb free and 11% Sb SQWs are shown in Fig. 6. For an increase in Sb composition from 0% to 11%, the depth of the hole QW increases by factor of ~5 (~200 meV) while the depth of the electron QW varies by less than 20% (~50 meV). In addition, the strain in the QW changes from tensile to compressive with an increase in Sb composition. The three samples shown in Fig. 2 correspond to tensily strained (3% Sb), nearly unstrained (6% Sb), and compressively strained (11% Sb) GaNAsSb/GaAs SQWs.

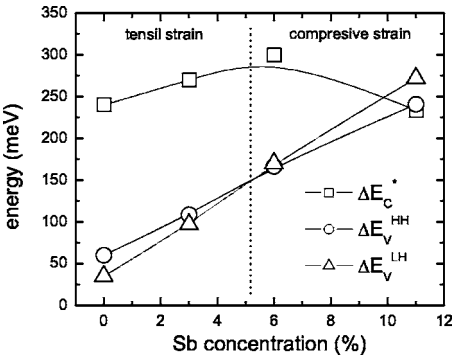

FIG. 6. Calculated variation of the electron ΔE_C^*, light-hole ΔE_V^{LH}, and heavy-hole ΔE_V^{HH} discontinuities for $GaN_{0.02}As_{0.98-x}Sb_x$/GaAs SQWs as a function of Sb composition.

However, for the three SQWs, the transition with the lowest energy is related to heavy hole due to the significant difference between heavy and light hole masses ($\sim 0.36\ m_0$ vs $\sim 0.09\ m_0$). For GaNAs/GaAs QWs, the transition related to the light hole is often not resolved in PR or CER spectra[23,24] because its intensity is typically weaker than the intensity of the transition related to the heavy hole. However, as it has been shown for tensily strained GaNAs (Ref. 2) and GaNAsSb (Ref. 10) layers, the fundamental band gap is between the light hole and conduction bands. PR resonances related to the light hole are clearly observed despite the fact that its intensity is weaker than the intensity of the transition related to the heavy hole. Therefore, we conclude that the transition related to the light hole must be considered in our CER spectra. However, for the $GaN_{0.02}As_{0.98-x}Sb_x$/GaAs SQW with 3% Sb, a clear observation of two separate resonances related to 11*H* and 11*L* is impossible due to the convolution of the 11*H* and 11*L* transitions ($\sim$9 meV) caused by broadening ($\sim$40–50 meV) of the CER resonance. The 11*H*-11*L* splitting increases with larger Sb content and a CER feature related to the 11*L* transition is clearly resolved for $GaN_{0.02}As_{0.98-x}Sb_x$/GaAs SQWs with 6% and 11% of Sb atoms, as shown in Fig. 2.

In addition to normally allowed transitions, such as 11*H*, 11*L*, and 22*H*, nominally forbidden transitions could be important for our samples due to factors including (i) imperfections in the squarelike profile of the QW, (ii) a surface electric field or (iii) a mixing of hole wave functions leading to a nonzero overlap of electron and hole wave functions for such transitions as 21*H*. However, the overlap is rather small and the oscillator strength for the nominally forbidden transitions is much smaller than that of ones allowed. Therefore these transitions are neglected in our fit (except the 32*H* transition for the $GaN_{0.02}As_{0.87}Sb_{0.11}$/GaAs SQW). However, it should be stated that CER features associated with these transitions can interfere with CER resonances related to allowed transitions (21*H* with 11*H* and 12*H* with 22*H*) because the energy separation between the first and the second heavy-hole levels is comparable to the broadening of the PR resonance ($\sim$45 meV vs $\sim$40–80 meV). The presence of weak CER features related to 21*H*, 31*H*, or 21*H* could be a reason for the broadening of CER resonances related to the 11*H* and 22*H* transitions is quite large. If we neglected the 32*H* transition and we fitted the spectrum from the 11% Sb QW with three resonances (similar to that of the QW with 6% Sb) we obtain the same energies for 11*H* and 11*L* transitions and different energy for the 22*H* transition. In the end, we fitted the CER spectrum of the 11% Sb QW sample with four resonances. The introduction of the fourth resonance is fully justified because the rise of Sb content causes the band gap energy of GaNAsSb to decrease ($\sim$17 meV per 1% of Sb). This leads to a redshift of the 11*H* and 22*H* transitions, as is seen in Fig. 2. In addition a third energy level appears for heavy holes and hence the 32*H* transition appears between resonances related to 22*H* and GaAs-related transitions.

CER measurements at low temperatures did not help to separate CER resonances in a significant manner. As it has been shown in Ref. 42, the broadening of QW transitions for a GaInNAs/GaAs SQW is very similar at 10 K and room temperature. Similar behavior has been observed for samples investigated in this article. This phenomenon is typical of III-V-N compounds and is associated with large alloy inhomogeneities for this material system. Finally, the low temperature CER (or PR) spectra of GaNAsSb/GaAs SQWs are comparable to CER (PR) spectra measured at room temperature. Therefore only room temperature CER spectra are analyzed in this article.

The observation of interband transitions related to excited states, such as 22*H* or 32*H*, confirms that $GaN_{0.02}As_{1-x}Sb_x$/GaAs QWs with $0<x\leqslant 0.11$ are type I. An interesting observation in this material system is the large sensitivity of Q_c to the Sb concentration. For SQWs shown in this article, we were able to tune the Q_C from 80% to 50% with only an increase in Sb composition from 0% to 11%.

V. CONCLUSIONS

Interband transitions in $GaN_{0.02}As_{0.98-x}Sb_x$/GaAs SQWs with $0<x\leqslant 0.11$ have been investigated by CER spectroscopy. The ground 11*H* and 11*L* transitions and the excited state transitions such as 22*H* and 32*H* were observed in the CER spectra. The experimental QW transition energies were compared with theoretical predictions based on an effective mass formalism model. The Q_C was varied to obtain a match between theory and measured data. It has been concluded that the Q_C decreases from 80% to 50% with an increase in Sb content from 0% to 11%. It corresponds to an increase of the depth of the hole QW by factor of 5 ($\sim$200 meV) and a variation of the depth of the electron QW is less than 20% ($\sim$50 meV). These results demonstrate that the band gap discontinuity in the GaNAsSb/GaAs material system is very sensitive to Sb composition and can be simply tuned by a change in this composition.

ACKNOWLEDGMENTS

We acknowledge support from the Foundation for Polish Science and the Stanford Network Research Center. H. B. Y. acknowledges support from the Stanford Graduate Fellowships.

*Present address: Solid State and Photonics Laboratory, Department of Electrical Engineering, 311X CISX, Via Ortega, Stanford University, Stanford, California 94305-4075, USA. Electronic address: kudrawiec@snow.stanford.edu

[1] I. A. Buyanova and W. M. Chen, *Physics and Applications of Dilute Nitrides* (Taylor & Francis, New York, 2004).
[2] M. Henini, *Dilute Nitride Semiconductors* (Elsevier, Oxford, 2005).
[3] G. Ungaro, L. Roux, R. Teissier, and J. C. Harmand, Electron. Lett. **35**, 15 (1999).
[4] J. C. Harmand, G. Ungaro, J. Ramos, E. V. K. Rao, G. Saint-Girons, R. Teissier, G. Le Roux, L. Largeau, and G. Patriarche, J. Cryst. Growth **227-228**, 553 (2001).
[5] J. C. Harmand, A. Caliman, E. V. K. Rao, L. Largeau, J. Ramos, R. Teisser, L. Travers, G. Ungaro, B. Theys, and I. F. L. Dias, Semicond. Sci. Technol. **17**, 778 (2002).
[6] F. Bousbih, S. Ben Bouzid, R. Chtourou, F. F. Charfi, J. C. Harmand, and G. Ungaro, Mater. Sci. Eng., C **21**, 251 (2002).
[7] S. A. Lourenco, I. F. L. Dias, L. C. Pocas, J. L. Duarte, J. B. B. de Oliveira, and J. C. Harmand, J. Appl. Phys. **93**, 4475 (2003).
[8] R. T. Senger, K. K. Bajaj, E. D. Jones, N. A. Modine, K. E. Waldrip, F. Jalali, J. F. Klem, G. M. Peake, X. Wei, and S. W. Tozer, Appl. Phys. Lett. **83**, 5425 (2003).
[9] L. H. Li, V. Sallet, G. Patriarche, L. Largeau, S. Bouchoule, L. Travers, and J. C. Harmand, Appl. Phys. Lett. **83**, 1298 (2003).
[10] H. B. Yuen, S. R. Bank, M. A. Wistey, J. S. Harris Jr., M.-J. Seong, S. Yoon, R. Kudrawiec, and J. Misiewicz, J. Appl. Phys. **97**, 113510 (2005).
[11] G. M. Peake, K. E. Waldrip, T. W. Hargett, N. A. Modine, and D. K. Serkland, J. Cryst. Growth **261**, 398 (2004).
[12] H. B. Yuen, S. R. Bank, M. A. Wistey, A. Moto, and J. S. Harris, Jr., J. Appl. Phys. **96**, 6375 (2004).
[13] R. Kudrawiec, K. Ryczko, J. Misiewicz, H. B. Yuen, S. R. Bank, M. A. Wistey, H. P. Bae, and James S. Harris Jr., Appl. Phys. Lett. **86**, 141908 (2005).
[14] S. Sakai, Y. Ueta, and Y. Terauchi, Jpn. J. Appl. Phys., Part 1 **32**, 4413 (1993).
[15] L. Bellaiche, S.-H. Wei, and A. Zunger, Phys. Rev. B **56**, 10233 (1997).
[16] K. Kitatani, M. Kondow, T. Kikawa, Y. Yazawa, M. Okai, and K. Uomi, Jpn. J. Appl. Phys., Part 1 **38**, 5003 (1999).
[17] M. Kozhevnikov, V. Narayanamurti, C. V. Reddy, H. P. Xin, C. W. Tu, A. Mascarenhas, and Y. Zhang, Phys. Rev. B **61**, R7861 (2000).
[18] I. A. Buyanova, G. Pozina, P. N. Hai, W. M. Chen, H. P. Xin, and C. W. Tu, Phys. Rev. B **63**, 033303 (2001).
[19] B. Q. Sun, D. S. Jiang, X. D. Luo, Z. Y. Zu, Z. Pan, L. H. Li, and R. H. Wu, Appl. Phys. Lett. **76**, 2862 (2002).
[20] P. Krisprin, S. G. Spruytte, J. S. Harris, and K. H. Ploog, J. Appl. Phys. **88**, 4153 (2000).
[21] P. Krisprin, S. G. Spruytte, J. S. Harris, and K. H. Ploog, J. Appl. Phys. **90**, 2405 (2001).
[22] P. J. Klar, H. Gruning, W. Heimbrodt, J. Koch, W. Stolz, P. M. A. Vicente, A. M. Kamal-Saadi, A. Lindsay, and E. P. O'Reilly, Phys. Status Solidi B **223**, 163 (2001).
[23] S. Tomic, E. P. O'Reilly, P. J. Klar, H. Gruning, W. Heimbrodt, W. M. Chen, and I. A. Buyanova, Phys. Rev. B **69**, 245305 (2004).
[24] R. Kudrawiec, M. Gladysiewicz, M Motyka, J. Misiewicz, J. A. Gupta, and G. C Aers, Solid State Commun. **138**, 365 (2006).
[25] R. Teissier, D. Sicault, J. C. Harmand, G. Ungaro, G. Le Rpux, and L. Largeau, J. Appl. Phys. **89**, 5473 (2001).
[26] R. Kudrawiec, G. Sek, K. Ryczko, J. Misiewicz, and J. C. Harmand, Appl. Phys. Lett. **84**, 3453 (2004).
[27] J. B. Wang, S. R. Johnson, S. A. Chaparro, D. Ding, Y. Cao, Yu. G. Sadofyev, Y.-H. Zhang, J. A. Gupta, and C. Z. Guo, Phys. Rev. B **70**, 195339 (2004).
[28] F. H. Pollak, in *Modulation Spectroscopy of Semiconductors and Semiconductor Microstructures Handbook on Semiconductors*, edited by T. S. Moss (Elsevier Science, Amsterdam, 1994), Vol. 2, pp. 527–635.
[29] F. H. Pollak and H. Shen, Mater. Sci. Eng., R. **10**, 275 (1993).
[30] R. C. Tu, Y. K. Su, D. Y. Lin, C. F. Li, Y. S. Huang, W. H. Lan, S. L. Tu, S. J. Chang, S. C. Chou, and W. C. Chou, J. Appl. Phys. **83**, 1043 (1998).
[31] M. Munoz, H. Lu, X. Zhou, M. C. Tamargo, and F. H. Pollak, Appl. Phys. Lett. **83**, 1995 (2003).
[32] R. Kudrawiec, P. Sitarek, J. Misiewicz, S. R. Bank, H. B. Yuen, M. A. Wistey, and James S. Harris Jr., Appl. Phys. Lett. **86**, 091115 (2005).
[33] R. Kudrawiec, M. Gladysiewicz, M. Motyka, J. Misiewicz, H. B. Yuen, S. R. Bank, M. A. Wistey, H. P. Bae, and James S. Harris Jr., Appl. Surf. Sci. (to be published).
[34] G. L. Bir and G. Pikus, *Symmetry and Strain-Induced Effects in Semiconductors* (Wiley, New York, 1974).
[35] I. Vurgaftman, J. R. Meyer, and L. R. Ram-Mohan, J. Appl. Phys. **89**, 5815 (2001).
[36] W. Shan, W. Walukiewicz, J. W. Ager III, E. E. Haller, J. F. Geisz, D. J. Friedman, J. M. Olson, and S. R. Kurtz, Phys. Rev. Lett. **82**, 1221 (1999).
[37] D. E. Aspnes, Surf. Sci. **37**, 418 (1973).
[38] H. Shen, X. C. Shen, F. H. Pollak, and R. N. Sacks, Phys. Rev. B **36**, 3487 (1987).
[39] G. Arnaud, P. Boring, B. Gil, J.-C. Garcia, J.-P. Landesman, and M. Leroux, Phys. Rev. B **46**, 1886 (1992).
[40] M. Galluppi, L. Geelhaar, H. Riechert, M. Hetterich, A. Grau, S. Birner, and W. Stolz, Phys. Rev. B **72**, 155324 (2005).
[41] P. N. Hai, W. M. Chen, I. A. Buyanova, H. P. Xin, and C. W. Tu, Appl. Phys. Lett. **77**, 1843 (2000).
[42] R. Kudrawiec, G. Sek, K. Ryczko, J. Misiewicz, P. Sundgren, C. Asplund, and M. Hammar, Solid State Commun. **127**, 613 (2003).